Corrosion Performance of Wire Arc Deposited Zinc Aluminum Pseudo Alloy and Zinc 15 Aluminum Alloy Coatings on Steel in Chloride Environment

Ratna Divya Yasoda¹, Ying Huang^{1*}, and Xiaoning Qi²

¹ Department of Civil, Construction and Environmental Engineering., North Dakota State University, Fargo, USA

Email: ratna.yasoda@ndus.edu; ying.huang@ndsu.edu

² Department of Coatings and Polymeric Materials, North Dakota State University, Fargo, USA

Email: xiaoning.qi@ndsu.edu.

* Corresponding author

Abstract

This study investigated the corrosion performance of wire arc deposited zinc-aluminum pseudo

alloy coating (Zn-Al pseudo alloy) with higher aluminum content and Zn-15Al alloy coating in

the aggressive chloride environment. The performance of both coatings was assessed by

employing morphological analysis, chemical composition and material characterization tests, and

electrochemical studies. Micrographs of the as-deposited coatings revealed a denser and compact

microstructure in the pseudo alloy coating compared to Zn-15Al coating. The electrochemical test

results demonstrated that the pseudo alloy coating exhibited a four times lower corrosion rate and

four times higher corrosion resistance compared to the Zn-15Al coating. Although, the formation

of simonkolleite is noticed in the corrosion products of both the coatings, a more thin and compact

corrosion product layer is observed in the pseudo alloy coating. The superior performance of Zn-

Al pseudo alloy coating can be attributed to the presence of higher aluminum content and the

existence of zinc-rich and aluminum-rich areas in the coating microstructure, where zinc offers

sacrificial protection at the aluminum-rich region boundaries, in addition to the formation of stable

corrosion products of zinc at zinc-rich areas, passivation of aluminum at the aluminum-rich areas,

reduced the overall rate of corrosion in such coatings.

Keywords: Thermally sprayed sacrificial coatings; Wire arc coatings; ASTM A36 structural steel;

Offshore structures; Marine environment; Corrosion mitigation.

1

Introduction

Steel is one of the most popular construction materials owing to its superior properties such as ductility, high strength to weight ratio, and good machineability to attain specific engineering needs (Ref 1). However, corrosion-induced degradation in steel structures has always been a major concern. Specifically, steel structures located in the marine or offshore environments encounter aggressive chlorides, which cause severe degradation in the steel (Ref 2-5). Additionally, steel infrastructure and transportation facilities such as bridges and roadways in the cold regions are also exposed to hostile chloride ions from de-icing salts during the winter season (Ref 6,7). Therefore, corrosion mitigation of the steel structures in the chloride-containing environment has become the main objective of extensive research among the scientific community around the globe.

Among several methods, protective coatings are considered to be a practical and most widely applied surface treatment to prevent corrosion in steel structures (Ref 8,9). Coatings produced from metals that are anodic to steel, such as zinc, aluminum, are very promising and attractive since these coatings offer both barrier and cathodic protection to substrate steel (Ref 10,11). With the combined cathodic nature and the barrier protection offered by the formation of stable corrosion products on the surface, minor coating discontinuities that can occur during transportation and erection of the structural steel members can be taken care of, which eliminates the need for pinhole-free coating layers (Ref 12,13). The attractive corrosion protection offered by coatings of zinc and aluminum makes these coatings a popular surface treatment method to protect steel structures in industrial and marine environments (Ref 14-16).

Although pure zinc and pure aluminum coatings offer good corrosion protection to steel, they have some limitations. Based on previous research, pure zinc coatings are found to exhibit

poor long-term performance in the marine environment, and pure aluminum coatings are demonstrated to be prone to pitting when exposed to a chloride-rich environment (Ref 17,18). To address these shortcomings, Zn-Al coatings have been introduced and became popular as they demonstrated better corrosion resistance compared to pure zinc or pure aluminum coatings (Ref 19,20).

Zn-Al coatings are applied either through hot-dip galvanizing (HDG) (Ref 21,22) or through thermal spraying (metalizing) (Ref 23). Among several thermal spraying techniques, flame spray process and wire arc spray process are ideal candidates for the application of Zn-Al coatings (Ref 24), as other spray processes involve either very high temperatures (4000° C to 15,000° C) or very high particle velocities (700 to 1000 m/s) or a combination of these two which are not favorable for the deposition of zinc and aluminum coatings (Ref 25). Specifically, the wire arc spray process has some unique advantages such as high deposition efficiency, low power input requirement, spray on-site flexibility for repairs and rehabilitation, and can be operated at low costs compared to other thermal spray processes (Ref 26,27). The advantages of the wire arc spray process and its suitability to apply anti-corrosive coatings of zinc and aluminum have led to the commercialization of the process lately (Ref 28).

Some of the earlier field studies conducted on thermally sprayed Zn-Al coatings showed that the Zn-Al alloy coatings outperformed pure zinc and pure aluminum coatings. For instance, an 18-year exposure test conducted by Kuroda et al. (Ref 29) in the marine environment on flame sprayed zinc, aluminum, and Zn-13Al coatings (87% Zn, and 13% Al by wt.) with and without sealants showed that Zn-13Al offered overall better protection compared to pure zinc and pure aluminum coatings with sealant. Moreover, some studies indicated that Zn-Al coatings produced by thermal spray process in which the aluminum content ~15 wt.% exhibited better corrosion

performance compared to pure metallic coatings (Ref 19,30). In addition, some researchers also investigated the influence of sulfate-reducing bacteria (SRB) on the corrosion behavior of wire arc sprayed zinc, aluminum, and Zn-15Al coatings in the seawater. The results of one such study suggest that compared to pore sealed zinc coating, pore sealed aluminum coating showed better performance in the presence of SRB in seawater, due to the formation of dense Al₂O₃ film along with the formation of thick biofilm which effectively reduced the intrusion of the corrosive medium into the aluminum coating (Ref 31). Another study conducted by Hong, Sheng, et al. (Ref 32) on sealed and unsealed Zn-15Al coatings in seawater in the presence of SRB concluded that the corrosion protection of Zn-15Al coating is by combined cathodic action and sealing effect of corrosion products, such as ZnS which plugs the coating pores and reduces the rate of corrosion. Therefore, Zn-15Al coatings became a popular coating composition to protect the steel in offshore and marine environments.

However, recently, the performance of thermally sprayed Zn-Al coatings with even higher aluminum content, i.e., more than 15%, gained the attention of researchers. Katayama et al. (Ref 33) investigated the corrosion protection performance of flame sprayed Zn, Al, Zn-30Al (70% Zn, and 30% Al by wt.) coatings in the marine environment for 33 years and concluded that Zn-30Al coating exhibited better corrosion protection. Overall, the better performance of Zn-Al coatings was attributed to the formation of compact corrosion product layer, which improved the performance compared to pure zinc or aluminum coatings. Nevertheless, achieving an aluminum content of more than 15 wt.% in Zn-Al alloy coatings using wire arc spray process is unfeasible since alloying of Zn-Al wires with more than 15 wt.% of aluminum lead to the formation of brittle intermetallic phases of aluminum during the alloying process (Ref 34). This is the other reason

why the Zn-15Al (85% Zn and 15% Al by wt.) coatings are widely applied through the wire arc spray process.

To overcome the limitation of the wire arc process for higher aluminum contents, few researchers investigated the corrosion behavior of wire arc-produced pseudo alloy coating of Zn-Al. The pseudo alloy coating is formed by the simultaneous melting and subsequent deposition of pure zinc and pure aluminum wires in the arc spray system instead of using alloyed wires on both sides of the arc gun as shown in Fig. 1. A compressed air stream accelerates the molten droplets towards the substrate and forms a coating. Hence, Zn-Al coatings with aluminum weight content greater than 15% can be produced practically. Lee et al. (Ref 35) studied wire arc sprayed Zn-Al pseudo alloy coating with 68 wt.% zinc and 28 wt.% aluminum to affirm that the pseudo alloy coating offers reliable corrosion protection to the substrate steel during prolonged immersion in 3.5 wt.% NaCl solution. In another research, Hu et al. (Ref 36) compared the corrosion protection performance of patented Zn-Al alloy coatings using wire arc with three different mass fractions of aluminum, 15%, 30%, and 50%. They found out that the Zn-30Al pseudo alloy coating exhibited the lowest corrosion rate. However, the alloying technology developed by Hu et al. is not commercially available. Moreover, in general alloying of metals involve a lot of time, cost, effort and causes environmental pollution. To sum up, the existing literature suggests that a composite coating of Zn-Al with higher aluminum content produced through pseudo alloying has many advantages over coatings produced from pre-alloyed wires.

Despite the fact that a substantial amount of work has been taken place in the field of corrosion behavior of thermally sprayed sacrificial coatings, an evident knowledge gap exists on how the corrosion mechanism in pseudo alloy coating is different from the alloyed coating and what is responsible for the improved performance of Zn-Al pseudo alloy coating compared to the

Zn-15Al coating, which is not available in the literature. The present work is an attempt to address this research gap. In view of this, a systematical experimental study has been carried out to investigate the corrosion performance and protection mechanism of Zn-Al pseudo alloy coating, and Zn-15Al alloy coatings deposited using the wire-arc spray process. In this study, in-lab accelerated corrosion tests were performed using neutral salt spray on coated ASTM A36 steel plates with the Zn-Al pseudo alloy and Zn-15Al alloy coatings. The corrosion performance was quantified by studying the corrosion products, penetration of chloride ions, and extent of oxidation with the help of various analytical techniques, such as field emission scanning electron microscopy (FE-SEM) equipped with energy dispersive spectroscopy (EDS) and X-ray diffraction (XRD) analysis. In addition, the electrochemical parameters such as corrosion current, corrosion potential, and corrosion rate were evaluated using the potentiodynamic polarization scanning (PDS) technique, and the impedance of the corrosion products were measured using the electrochemical impedance spectroscopy (EIS) method. For the remainder of the manuscript, Zn-15Al alloy coating is referred to as Zn-15Al coating, and Zn-Al pseudo alloy coating is referred to as pseudo alloy coating for simplicity.

2. Wire Arc Sprayed Zn-Al Coatings and Corrosion Characterization Methods

This section details the coating application procedure to produce pseudo alloy and Zn-15Al coatings using wire arc spraying, protocols for accelerated corrosion tests to corrode the coatings, corrosion performance characterization tests, and microstructural analyses on the coatings.

2.1 Coating Procedure for Zn-Al pseudo alloy and Zn-15Al alloy coatings

To produce the pseudo alloy coating, 99% pure zinc and 99% pure aluminum wires of diameter 1.6 mm each was used as feedstock materials. For the Zn-15Al coatings, commercially

available Zn-15Al wires of diameter 3.175 mm were used as feedstock materials in the wire arc spray gun. Before the coating deposition, the ASTM A36 substrates were grit blasted using alumina to ensure good coating adhesion. Fig. 1 shows the spray gun used for the process, and Table 1 shows the process parameters used during the wire arc coating process. The process parameters used in the present work, represent values at which a stable arc was generated, and a smoother coating deposition process was achieved with the considered diameter of the wires, in the spray gun. These values are also in close agreement with the values reported in the literature (Ref 13,14,30,37-40). The measured average roughness (R_a) of both the coatings in the asdeposited condition is $\sim 6 \pm 0.5 \ \mu m$.

2.2 Accelerated Corrosion Test Setup

Accelerated corrosion tests were performed on the wire arc deposited pseudo alloy and Zn-15Al coatings by employing neutral salt spray to simulate the marine conditions with a chloride environment. The temperature of the salt spray chamber was maintained at 35±2°C and 100% relative humidity as per ASTM B117-97 (Ref 41) guidelines. Before placing the samples in the chamber, the uncoated edges and back of the steel samples were carefully masked to prevent the initiation of crevice corrosion from the edges. The specimens were exposed to 400 hours of salt spray at which the formation of corrosion products on the coating surface had become noticeable.

2.3 Microstructural Characterization of the Coatings

Microstructural evaluation of both as-sprayed and corroded pseudo alloy and Zn-15Al coatings was performed to quantify the elemental composition and through-thickness distribution of zinc, aluminum, geometric defects, including pores and splats that strongly influence the corrosion performance of the coatings. The coating defects, surface, and cross-section

morphologies of the as-sprayed coatings and coatings after being subjected to neutral salt spray were examined using a field emission scanning electron microscope (FE-SEM) operated at 15kV (JEOL JSM-7600F). This instrument was equipped with energy-dispersive X-ray spectroscopy (EDS) tool for elemental analysis. The corrosion products on the coating surface had been stabilized by impregnating them with epoxy resin and were polished as per the standard guidelines (Ref 42) prior to the SEM analyses. Please note that the micrographs presented in this study are obtained at different magnifications (see Figs. 2,3,5 and 6) to capture the most important cross-sectional and surface features which have varying dimensions. Any statements on comparisons are made keeping in view the scale marked on each of the micrographs that are being discussed and hence the influence of magnification at which the micrographs are obtained had no bearing on the results and discussion.

To identify the phases, present in the unexposed coatings as well as in the corrosion products, the X-ray diffraction (XRD) technique was used to evaluate the phase composition of the pseudo alloy and Zn-15Al coatings before and after being subjected to neutral salt spray. The XRD was carried out using (Bruker D8 discover X-ray Diffractometer) Cu Kα radiation generated at 40kV and 40 mA.

2.4 Corrosion Performance Tests

Potentiodynamic polarization scanning (PDS) and electrochemical impedance spectroscopy (EIS) were conducted on both the coatings that were exposed to neutral salt spray to characterize the corrosion performance of the coatings. PDS was carried out on both the coatings before, during, and after being subjected to neutral salt spray to compare the changes in corrosion current with the increase in exposure time to neutral salt spray.

Additionally, to understand the difference in electrochemical nature of the corrosion product layer formed on both pseudo alloy and Zn-15Al coatings, EIS was run on the coatings after being subjected to neutral salt spray. In the electrochemical study (both PDS and EIS), a minimum of three replicates of both coatings were tested for each of the test conditions to ensure repeatability of results. All the samples were cleaned thoroughly, degreased with ethanol, and rinsed with distilled water, and blow-dried prior to the tests. A three-electrode system with coating surface as working electrode, platinum wire mesh as the counter electrode, and saturated calomel electrode (SCE) as reference electrode were used to make the corrosion cell for both the PDS and EIS analyses. The working electrode area was 1 cm² in the study and 3.5 wt.% NaCl solution was used as an electrolyte in the corrosion cell. The corrosion cell was placed in the Faraday cage to shield the electrochemical test set up from external electromagnetic interference. A Gamry potentiostat (Reference 600) was employed to carry out the electrochemical studies. PDS was run with a scan rate of 1 mV/s from -0.4 to +0.8 V with respect to open circuit potential (OCP). The EIS measurements were taken by changing the frequency of 3 mV sinusoidal voltage from 100kHz to 10 mHz.

3. Results and Discussion

3.1 Morphology and Chemical Composition of As-sprayed Coatings

Morphology in the present study refers to the visual appearance of the coating surface and cross-section at the microscale level. Figs. 2(a~c) and 3(a~c) show the FE-SEM images of the pseudo alloy and Zn-15Al coating surfaces and cross-sections in the as-sprayed condition, respectively. Microstructural features with sizes greater than 50 μm can be distinguished in these SEM images and no such distinctive surface morphological features were found on the surface micrographs of both coatings. Based on the visual appearance of their cross-sections, both coatings

have good adherence to the substrate steel with a coating thickness ranging between 250 to 300 μ m for the pseudo alloy coating and from 400 to 450 μ m for the Zn-15Al coating.

Based on the visual observation of the cross-sectional micrographs of the pseudo alloy coating in Figs. 2(b) and (c), the coating microstructure comprises a dark grey and light grey lamella overlapping alternatively. The dark grey regions are the aluminum-rich areas, and the light grey regions are the zinc-rich areas. The boundary between the aluminum-rich and zinc-rich areas is also seen. On the other hand, the microstructure of the Zn-15Al coating exhibited a lamellar structure comprising of thin layers of coating overlapping each other. There are no aluminum-rich and zinc-rich areas and no clear boundary between the two different metals as it was sprayed from an alloyed wire (see Figs. 3(b) and (c)). However, pores and splat boundaries between coating layers are apparent in the cross-sectional micrographs, as shown in Fig. 3(c), which is an inherent property of the thermal spray coatings, caused by the uneven overlap of the metal droplets (Ref 13,16). When comparing Figs. 2(c) and 3(c), it can be found that the presence of pores was not obvious in the pseudo alloy coating while it was apparent in the Zn-15Al coating. The individual metal droplets of zinc and aluminum might have achieved full deformation and a high degree of flattening during the spray deposition process in the case of pseudo alloy coating, resulting in a more dense and compact microstructure when compared to Zn-15Al coating (Ref 40).

Based on the surface and cross-sectional micrographs of both coatings shown in Figs. 2 and 3, a simplified idealization of the micrographs of both coatings is illustrated in Fig. 4(a~c). Specifically, Fig. 4(c) illustrates the boundaries between the aluminum-rich and zinc-rich areas. Thus, for the pseudo alloy coatings, multiple corrosion protection mechanisms may be active, including 1) dissolution of zinc protecting zinc-rich regions, 2) dissolution followed by passivation of aluminum protecting aluminum-rich regions, and 3) an additional sacrificial dissolution of zinc

that protects the aluminum at the zinc-aluminum boundaries that synergistically protects the substrate metal. While for the Zn-15Al coatings, the coating matrix looks homogeneous without clusters of aluminum-rich and zinc-rich areas as shown in Fig. 4(a) and the corrosion protection mechanism is predominantly due to the active dissolution of the zinc and aluminum, which forms relatively stable corrosion products that protect the coating from further dissolution. Thus, the pseudo alloy coatings with more or less the same aluminum content as that of the alloy coatings are also demonstrated to have better corrosion performance when compared to the alloy coatings (Ref 34) due to the presence of an additional corrosion protection mechanism, aka additional sacrificial dissolution of zinc at the zinc-aluminum boundaries.

The chemical composition of the pseudo alloy and Zn-15Al coatings was obtained from the EDS analysis from six different locations on the cross-section of both coatings. Table 2 summarizes the average elemental composition for both coatings. The Zn-15Al coating was composed of 17.08 wt.% of aluminum and 79.78 wt.% of zinc which is very close to the actual composition of the feedstock wire. The Zn-Al pseudo alloy coating consisted of 37.21 wt.% of aluminum and 58.46 wt.% of zinc, although both aluminum and zinc wires were sprayed simultaneously at the same rate. Similar high zinc content in pseudo alloys was reported in a recent study (Ref 35). This can be attributed to the low density of aluminum (2,700 kg/m³) which is around 2.64 times less compared to the density of zinc (7,135 kg/m³). Furthermore, the melting point of zinc (419.5°C) is lower than aluminum (660.3°C) which might have an impact on the viscosity of the molten metal droplets that can result in an altered deposition rate. The exact reason for the difference in the composition is not investigated in this study as it falls outside the scope of the current work. Finally, the presence of 3 to 4 wt.% of oxygen in the coating composition was observed, which can be due to the oxidation of coating material during the wire arc spray process

(Ref 40). When the aluminum weight percentage is lower than 50% in Zn-Al alloys, the Zn-Al coatings with higher aluminum content are found to be better than coatings with lower aluminum content (Ref 42-43). Thus, with both additional corrosion protection mechanisms and higher aluminum contents, the pseudo alloy coating may show superior corrosion performance compared to the commonly used Zn-15Al coating.

3.2 Morphology of the Coatings after Accelerated Corrosion

To investigate the corrosion performance of both coatings, SEM images were taken on the surface, and cross-section and EDS analysis was carried out on the corroded coatings. The surface micrographs of the corroded specimens provide helpful information about the extent of corrosion and the presence of cracks and pores on the coating surface that are responsible for the ingress of electrolyte solution into the coating. At the same time, the cross-section micrograph of the corroded coatings reveals the affected thickness of the coating and the depth of the corrosion product layer formed on the surface during the neutral salt spray exposure. Additionally, EDS analysis on the cross-section gives crucial information about all the elements in the corroded coatings, especially the chloride ions distribution and their penetration depth, and the severity of oxidation in the coating layers.

Figs. 5(a, b) and 6(a, b) show the surface and cross-sectional micrographs of the pseudo alloy and Zn-15Al coatings after neutral salt spray, respectively. The surface micrographs of the pseudo alloy coating indicated the formation of a dense layer of corrosion products with very few micro-cracks on the coating surface, as shown in Fig. 5(a). The cross-sectional micrograph of the corroded pseudo alloy coating in Fig. 5(b) indicated that the formed corrosion product layer is very thin with an average thickness of around 25 μm. In addition, no ingress of electrolyte, and minimal oxidation was observed beyond this thin corrosion product layer into the coating, confirmed by

the EDS maps of chloride ions and oxygen respectively, demonstrating the compactness of the oxidized layer (see Fig. 7(c) and 7(d)). In addition, the lower corrosion current, and higher impedance values obtained from electrochemical tests on the corroded coatings (after 400 hrs of salt spray), reiterated the adherent and protective nature of the corrosion products formed, in the pseudo alloy coating. This superior performance with minimal penetration of chloride ions can be attributed to the fact that aluminum-rich areas form a very thin (~4 nm) passive oxidation layer when exposed to a corrosive medium (Ref 27) and the selective/minimal dissolution of zinc in the zinc-rich areas which may form relatively stable corrosion products of zinc (Ref 35). Moreover, zinc is more electronegative compared to aluminum and offers sacrificial protection to aluminum at Zn-Al boundaries. The combined action of the three mechanisms described in section 3.1 played an essential role in reducing the overall dissolution of the coating in the case of pseudo alloy coating.

On the other hand, in the case of Zn-15Al coatings, as shown in Fig. 6(a), the corroded coating surface was covered with a thick layer of corrosion products with numerous cracks and holes, and the corresponding cross-sectional micrograph of the coating in Fig. 6(b) showed the formation of ~240 µm thick corrosion products. This can be due to the active dissolution of zinc, which is the major constituent (85 wt.%) in the Zn-15Al coating. Moreover, earlier studies show that zinc forms expansive oxides and hydroxides such as ZnO, Zn(OH)₂, ZnOHCl (Ref 20,33,43-45) during the corrosion in the chloride environment, which might have resulted in the formation of a thicker corrosion product layer (Fig. 6(b)) in Zn-15Al coating compared to pseudo alloy coating (Fig. 5(b)).

Elemental distributions obtained from EDS analysis of the cross-sections of corroded coatings of pseudo alloy and Zn-15Al coatings are shown in Figs. 7 and 8, respectively.

Specifically, Figs. 7(a, b) and 8(a, b) show the distribution of zinc and aluminum in pseudo alloy and Zn-15Al coatings, respectively. The zinc-rich areas and aluminum-rich areas are visible in the EDS maps for the pseudo alloy coating, as shown in Figs. 7(a) and (b). On the other hand, zinc and aluminum are found to be uniformly distributed in the coating thickness in the case of Zn-15Al coatings, as seen in Figs. 8(a) and (b). The EDS analysis corroborates the distribution of Zn and Al within the coatings inferred from SEM analyses of the coating cross-sections (see Figs. 2 and 3). The presence of zinc and aluminum-rich islands in the pseudo alloy coating is due to the use of separate zinc and aluminum wires, and the uniform distribution of zinc and aluminum in the Zn-15Al coating can be attributed to the use of alloyed wire, during the coating deposition process.

Figs. 7(c) and 8(c) show the distribution of oxygen in the cross-sections of the corroded pseudo alloy and Zn-15Al coatings, respectively. In the pseudo alloy coating, a high concentration of oxygen was observed only on the top layer of the corrosion products. The remaining thickness appeared to be not oxidized, as seen in Fig. 7(c). While for the Zn-15Al coating, oxygen concentration gradient was observed in the entire coating thickness, and the concentration of oxygen decreased with the increase in the depth of the oxidized layer as seen in Fig. 8(c), indicating that the regions near the substrate are less damaged when compared to the outermost oxidized layer.

Figs. 7(d) and 8(d) show the distribution of chlorides in the corroded pseudo alloy and Zn-15Al coatings, respectively. It can be seen that in the case of pseudo alloy coating, the chlorides remained in the corrosion product layer and confirmed the depth of the corrosion products (25 μm) inferred from SEM analysis (see Fig. 5(b)). Similarly, even in the case of Zn-15Al coating, chlorides are found to be distributed throughout the corrosion product layer, which is 240μm

confirming the corrosion product thickness obtained from SEM images (see Fig. 6(b)). The Zn-15Al coating showed a much deeper penetration of the chloride ions, which is 9.6 times deeper than the penetration of the chloride ions noticed in the pseudo alloy coating.

3.3 X-ray Diffraction Analysis of the Coatings

To determine the metallurgical phases and oxidation product composition, XRD analysis was performed on the pseudo alloy and Zn-15Al coatings in as-deposited conditions and after exposure to neutral salt spray. The corrosion protection performance of coatings depends on the nature of the metallurgical phases and mineral oxides, if any, present in the as-deposited coating surface, which directly encounters the corrosive environment. Besides, the composition of the corrosion products formed after being exposed to the corrosive environment provides valuable information to analyze the corrosion protection mechanism offered by the coatings.

Fig. 9 shows the XRD results obtained from as-deposited pseudo alloy and Zn-15Al coatings. Both the pseudo alloy and Zn-15Al coatings exhibited more or less the same diffraction pattern. According to the ICDD 2021 (International Center for Diffraction Data) database, only pure zinc (hexagonal close-packed – HCP) and pure aluminum (face-centered cubic – FCC) were present on the surfaces of both the coatings in uncorroded condition. Although EDS results indicated the presence of 3.15 wt.% and 4.33 wt.% of oxygen in Zn-15Al and pseudo alloy coatings, respectively, no oxygen peaks were observed in the XRD analysis eliminating the possibility of the presence of any mineral oxides. This discrepancy can result from either a local artifact of surface oxidation due to exposure to the atmosphere identified by the EDS or the low specificity of XRD that cannot quantify the presence of trace amounts of oxidative products on the coating (Ref 35). It should also be noted that the EDS and XRD analyses were performed on the cross-section and surface of the coating, respectively, considering the experimental constraints.

Figs. 10 and 11 illustrate the XRD pattern of corrosion products on the pseudo alloy and Zn-15Al coatings, respectively. There is a possibility of the formation of a wide range of loosely bound oxides, hydroxides, and chlorides of zinc and aluminum such as ZnO, Zn (OH)₂, ZnCl₂, Al₂O₃, Al (OH)₃ AlCl₃ when Zn-Al coatings are exposed to the marine environment (Ref 20,35,46). Since these products are loosely bound and dissolve in water, they were not found in the XRD analysis. However, stable corrosion products like simonkolleite and hydrozincite can be observed for zinc (Ref 35,47), and impenetrable and very thin (~4 nm) Al₂O₃ and Al (OH)₃ (Bayerite) can be observed in the case of aluminum (Ref 39,48). Fig. 10 shows the diffraction pattern of corroded pseudo alloy coating, and apart from zinc and aluminum, simonkolleite was found to be the only compound present in the corrosion products. On the other hand, the diffraction obtained from the corroded Zn-15Al coating correspond to simonkolleite (Zn₅(OH)₈Cl₂.H₂O) and hydrozincite (Zn₅(CO₃)₂(OH)₆) along with zinc and aluminum peaks, as shown in Fig. 11. Since the minerals, simonkolleite, and hydrozincite are relatively more stable corrosion products and are sparingly soluble in water at neutral pH values and hence were detected in the XRD analysis. The formation of simonkolleite during the corrosion of zinc in chloride atmosphere was reported in several earlier studies and emphasized that this stable corrosion product filled the coating pores and blocked the cathodic sites, thereby improving the corrosionresistant properties of the coating (Ref 12,33,35,36). The presence of hydrozincite in the corrosion products of zinc coatings was also reported in some studies (Ref 33). From the diffraction analysis of the corrosion products of both pseudo alloy and Zn-15Al coatings, it is apparent that the corrosion products resulted from the active dissolution of zinc-rich areas. No compound due to the dissolution of aluminum was observed in both coatings after 400 hours of neutral salt spray. Moreover, very few and low-intensity peaks of simonkolleite (corrosion product of zinc) were

observed in the corrosion products of pseudo alloy coating. This diffraction pattern in the present study reiterates that the pseudo alloy coating had undergone very little corrosion, which can be attributed to the selective dissolution of zinc in zinc-rich regions, and the cathodic protection of aluminum by zinc resulted in the formation of more corrosion products of zinc when compared to the aluminum which generally forms a thin passive layer of oxides in the order of few nanometers on the surface of the coating during accelerated corrosion (Ref 35,49).

3.4 Potentiodynamic Polarization Measurements

Zinc and aluminum have low oxidation potentials and hence undergo active degradation in chloride-containing environments (Ref 11,50). However, zinc forms stable corrosion products on the coating surface, such as simonkolleite and hydrozincite, as observed in the XRD study (refer to section 3.3) during the initial period of exposure, which slows down the dissolution process. Similarly, aluminum also forms a passive oxide layer when subjected to a corrosive environment that hinders the intrusion of electrolytes into the coating. The combined action of zinc and aluminum is responsible for the excellent corrosion protection performance of Zn-Al coatings on the structural steel. Therefore, in this study to demonstrate the role and efficacy of zinc-aluminum protection mechanisms in pseudo alloy and Zn-15Al coatings on steel when exposed to corrosive environments such as marine (or) offshore conditions, potentiodynamic polarization tests were conducted on both the coatings in unexposed conditions and after being subjected to 200 hours and 400-hour neutral salt spray. Figs. 12 and 13 show the corresponding polarization plots obtained for pseudo alloy and Zn-15Al coatings, respectively. Table 3 summarizes the electrochemical parameters, including corrosion potential and corrosion current obtained from Tafel extrapolation at different exposure durations.

Corrosion potential (E_{corr}) is the potential of the working electrode when no external current is applied or in other words when the overall anodic current is equal to the cathodic current which reflects the tendency of the coating surface to lose electrons in the presence of an electrolyte. The higher the E_{corr} value, the lesser the tendency to lose electrons and hence more resistant to corrosion damage (Ref 51). With the increase in the salt spray exposure time from 0 to 400 hours, the corrosion potential values moved to a nobler direction (less tendency for anodic dissolution) in both the pseudo alloy and Zn-15Al coatings. The E_{corr} value was increased from -1.25 to -1.11 V in the case of pseudo alloy coating and increased from -1.26 to -1.08 V in the case of Zn-15Al coating. The positive shift of potentials in the coatings can be attributed to the blocking of surface area by relatively non-soluble and stable corrosion products like simonkolleite and hydrozincite during the salt spray exposure (Ref 36). In both the coatings, the corrosion potential values were still well below the critical value -0.8 V vs. SCE, which indicates that both the coatings provided sacrificial protection to the steel during salt spray exposure (Ref 35,52).

Another critical parameter to estimate the corrosion protection performance of the coating is the corrosion current (i_{corr}). The corrosion current is directly proportional to the rate of corrosion of the coating and hence the life of the coating. For the pseudo alloy coating, the i_{corr} value increased only from 1.17 to 7.3 μ A/cm² when exposed to 200 hours of natural salt spray. More interestingly, the i_{corr} value was decreased again to 3.4 μ A/cm² at the end of 400 hrs. In a previous study on as-deposited ZnAl pseudo alloy coating with 28.12 wt.% aluminum an i_{corr} value of 7.19 μ A/cm² was reported (Ref 35). In another study on as-deposited Zn-30Al alloy coating with 30 wt.% aluminum, which was comparable to the pseudo alloy aluminum content used in the current study, reported an i_{corr} value of 27.7 μ A/cm² (Ref 36). On the other hand, in the case of Zn-15Al coating, the i_{corr} increased from 4.53 to 136 μ A/cm² with an increase in

exposure time from 0 to 400 hrs. A similar trend is observed in a past study where a Zn-Al alloy coating with 14 to 16 wt.% of aluminum is immersed in 3.5 wt.% NaCl solution for 500 hours (Ref 14).

From the above-mentioned studies in the literature, it is clear that the i_{corr} values are lower in the pseudo alloy coatings and also in the alloy coatings with higher aluminum weight percentages. In this study, we investigated a Zn-Al coating that jointly benefits from the pseudo alloying and a higher weight percentage ($\sim 37\%$) of aluminum. Hence, even better corrosion protection is anticipated. This explains the extremely low corrosion current even after exposure to 400 hours of neutral salt spray in the case of pseudo alloy coating. The decrease in the i_{corr} value beyond 200 hours of exposure to the neutral salt spray in the pseudo alloy coating can be attributed to the formation of an impenetrable oxide layer. This is corroborated by the EDS map of chlorides (see Fig. 7(d)), which indicated minimal chloride ion penetration in the case of pseudo alloy coating. At this juncture, it is also worth noting that the chloride ions were reported to aggressively break intact oxide layers in many metals, as shown in several previous studies (Ref 9,53-56). Once the corrosion current is obtained, the corrosion rate (μ m/year) can be estimated using the following equation derived from Faraday's law (Ref 57):

Corrosion rate (
$$\mu$$
m/year) = $\frac{3.27 \text{ x i}_{\text{corr}} \text{ x E.W}}{d}$ (1)

where i_{corr} ($\mu A/cm^2$) is the corrosion current obtained from Tafel extrapolation, E.W is the equivalent weight of the metal (grams/mole), and d is the density of the metal in (g/cm³). From Table 3, the pseudo alloys coating had a corrosion rate of 16.60 μ m/year in unexposed condition, which was almost four times lower than the corresponding Zn-15Al coating, which was 65.83 μ m/year. Compared to the bare steel, which is expected to have a corrosion rate of up to 250

μm/year in seawater (Ref 2,58), the Zn-15Al coating reduced the corrosion rate by 3.8 times, and the pseudo alloys coating reduced the rate of corrosion by 15 times. Since the density and equivalent weight of complex corrosion products formed on the surface of the coatings is not available, the corrosion rates of the coatings after 200 hours and 400 hours of salt spray exposure were not included in Table 3.

3.5 Electrochemical Impedance Spectroscopy (EIS) Measurements

In addition to the polarization measurements, the EIS technique is an effective tool to understand and distinguish different processes in electrochemical reactions over a wide range of frequencies. The material should be electrochemically stable with respect to OCP to employ this technique (Ref 59). Therefore, only a minimal perturbation of less than 10 mV is generally used to maintain the system in equilibrium, and less than 5 mV is recommended for metallic coatings (Ref 60). As a result, impedance spectrums are obtained by recording the impedance values (ratio of potential to the current) over the studied frequency range. One of the ways to visually present EIS results is the Nyquist plot, in which imaginary impedance (imaginary Z) representing the capacitive response is plotted against the real impedance (real Z) representing the resistive response of the system.

Fig. 14 shows the Nyquist plot obtained from the pseudo alloy and Zn-15Al coatings after exposure to salt spray. The Nyquist plot of both coatings shows two different semi-circle loops. The high-frequency loop corresponds to the coating. The low-frequency loop corresponds to the corrosion process, which is the oxide layer/solution interface produced due to the penetration of electrolyte through the pores that causes dissolution of active sites inside the coating (Ref 35,36). Although both coatings exhibited an identical behavior over the entire range of frequencies in the Nyquist plot, a much larger loop (higher diameter) is generated in the case of pseudo alloy coating.

A larger loop indicates better corrosion resistance of the coating in the considered corrosive medium (Ref 34). The higher impedance values in the case of pseudo alloy coating compared to the Zn-15Al coating indicates that Zn-Al pseudo alloy coating offers better corrosion resistance compared to Zn-15Al coating. This can be attributed to either effective deposition of corrosion products in the pores/defects or forming a passive protective layer at the metal solution interface for the pseudo alloy coating compared to the Zn-15Al coating which significantly decreases the active area for corrosion.

Another representation of impedance data to study the corrosion process is Bode modulus frequency and phase angle frequency plots, as seen in Figs. 15 and 16, respectively, for both coatings. The Bode modulus frequency plot (Fig. 15) provides the impedance values at different frequencies, especially the impedance value at the lower studied frequency corresponding to the oxide layer or corrosion product layer (Ref 36,40). The higher the impedance value at low frequency, the better corrosion protection offered by the corrosion products formed on the coating surface. The impedance value was $2067 \,\Omega$ -cm² for the pseudo alloy coating and $405 \,\Omega$ -cm² for the Zn-15Al coating, indicating the formation of a more protective, adherent, and uniform layer corrosion product in pseudo alloy coating compared to Zn-15Al coating after being exposed to natural salt spray.

In the Bode phase angle frequency plot (Fig. 16), two-phase angle peaks were observed corresponding to the two semi-circle loops in the Nyquist plot, showing that the system had two-time constants (Ref 61). The first phase angle peak appeared between 0.1 and 1 Hz for the pseudo alloy coating, and the second phase angle peak occurred at the higher frequencies (between 10Hz and 100Hz). The value was higher than the Zn-15Al coating, which had a weak second phase-angle peak, and both the peaks occurred at low frequencies (below 10Hz). The increase in phase

angle peak at the higher studied frequency indicated that the corrosion products were more protective and effectively blocked the electrolyte access into the coating (Ref 35,36).

The study's EIS results agree with the microstructure observations and polarization results and reiterate that the pseudo alloy coatings of Zn-Al by wire arc with higher aluminum content offers better corrosion protection to substrate steel compared to the Zn-15Al alloy coating in a chloride environment.

4. Conclusions

This paper compared the corrosion protection performance of the pseudo alloy coating of Zn-Al with higher aluminum content and Zn-15Al alloy coatings deposited using the wire arc spraying technique. Overall, the pseudo alloy coating showed a superior corrosion performance compared to Zn-15Al coating, due to a) the presence of higher aluminum content and b) the presence of zinc-rich and aluminum-rich areas in the coating microstructure. Based on the systematical experimental studies performed in this study, the following conclusions can be drawn:

- (1) After being subjected to 400 hours of neutral salt spray, the depth of the corrosion product layer was found to be less than 25 μm for the pseudo alloy coating and 240 μm for the Zn-15Al coating, indicating the formation of high volume corrosion products and active dissolution in Zn-15Al coatings when compared to the pseudo alloy coatings. Remarkably, the chlorides penetrated the entire depth of the corrosion product layer for both the pseudo alloy and Zn-15Al coatings signifying the deleterious effect of chlorides on the metal coating.
- (2) The corrosion potential (E_{corr}) was shifted to a positive direction in both the pseudo alloy and Zn-15Al coatings with an increase in natural salt spray exposure time from 0 to 400 hours,

- which can be attributed to the formation of a passive protective layer made of corrosion products on the coating surface.
- (3) For the pseudo alloy coating, the corrosion current increased from 1.17 μ A/cm² to 7.30 μ A/cm² with an increase in neutral salt spray exposure from 0 to 200 hours and then subsequently decreased to 3.40 μ A/cm² at the end of 400 hours due to the synergistic action of selective dissolution of zinc in zinc-rich regions, aluminum dissolution in aluminum-rich areas and cathodic protection offered by zinc at the Zn-Al boundaries, while for the Zn-15Al coating, the corrosion rate increased from 4.53 μ A/cm² to 136.00 μ A/cm² with the increase in salt spray exposure time from 0 to 400 hours, which can be attributed to the active dissolution of the coating.
- (4) The impedance of the oxidized layer was observed to be 2,067 Ω -cm² in the pseudo alloy coating and 405 Ω -cm² in the Zn-15Al coating, showing that the corrosion products formed on the surface of pseudo alloy coating exhibited higher corrosion resistance attributed to the stability of the formed oxide layer.
- (5) The XRD results confirmed the formation of simonkolleite for the pseudo alloy coating and simonkolleite and hydrozincite in the corrosion products of the Zn-15Al coating. No peaks corresponding to compounds of aluminum were identified as the aluminum oxide layers were extremely thin when compared to the zinc oxide layer and the domination of zinc dissolution in zinc-rich regions and cathodic protection of aluminum by zinc resulting in more zinc oxide compounds when compared to the aluminum compounds on the surface of the coating.

In the future, long-term field tests on pseudo alloy coatings in various corrosive environments, including industrial, offshore, and energy sectors, are necessary to confirm these coatings' superior corrosion protection. Furthermore, corrosion protection in sulfate-rich and corrosion-causing

microbe-rich environments is also essential to investigate the versatility of Zn- Al pseudo alloy coatings.

CRediT authorship contribution statement

Ratna: Data curation, Methodology, Formal analysis, Investigation, Writing - original draft, Writing - review & editing. Ying Huang: Project administration, Funding acquisition, Supervision, Writing - review & editing. Xiaoning Qi: Supervision, Writing - review & editing.

Declaration of interest

The authors declare that they have no known competing financial interests or personal relationships that could have appeared to influence the work reported in this paper.

Acknowledgments

This work was supported by the National Science Foundation under Grant No. CMMI-1750316. The findings and opinions expressed in this article are those of the authors only and do not necessarily reflect the views of the sponsors. In addition, the suppliers and point of contacts from Thermal Spray Depot (Washington, PA, USA) are gratefully acknowledged for providing materials and support.

References

- 1. K.A. Chandler, Marine and offshore corrosion, Elsevier, 1985
- 2. J.P. Ault, The use of coatings for corrosion control on offshore oil structures, *Journal of protective coatings & linings*, **23**(4), 42-46 (2006)
- 3. A. López-Ortega, R. Bayón, J. Arana, Evaluation of protective coatings for offshore applications. Corrosion and tribocorrosion behavior in synthetic seawater, *Surface and Coatings Technology*, **349**, 1083-1097 (2018)
- 4. M. Iannuzzi, A. Barnoush, R. Johnsen, Materials and corrosion trends in offshore and subsea oil and gas production, *npj Materials Degradation*, **1**(1), 1-11 (2017)
- 5. K.Y. Ann, H.-W. Song, Chloride threshold level for corrosion of steel in concrete, *Corrosion science*, **49**(11), 4113-4133 (2007)
- 6. H.U. Sajid, R. Kiran, Influence of corrosion and surface roughness on wettability of ASTM A36 steels, *Journal of Constructional Steel Research*, **144**, 310-326 (2018)
- 7. H.U. Sajid, R. Kiran, X. Qi, D.S. Bajwa, D. Battocchi, Employing corn derived products to reduce the corrosivity of pavement deicing materials, *Construction and Building Materials*, **263**, 120662 (2020)
- 8. F. Deng, Y. Huang, F. Azarmi, Y. Wang, Pitted corrosion detection of thermal sprayed metallic coatings using fiber Bragg grating sensors, *Coatings*, **7**(3), 35 (2017)
- 9. P.A. Sørensen, S. Kiil, K. Dam-Johansen, C.E. Weinell, Anticorrosive coatings: a review, *Journal of Coatings Technology and Research*, **6**(2), 135-176 (2009)
- 10. Y.-t. Li, B.-r. Hou, Anticorrosion Mechanism of Thermal Spraying Coatings of Zinc and Aluminum and of Alloys Made of the Same in Marine Environment: A Review, *MATERIALS PROTECTION-WUHAN-*, **38**(9), 30 (2005)
- 11. A. Farooq, M. Hamza, Q. Ahmed, K.M. Deen, Evaluating the performance of zinc and aluminum sacrificial anodes in artificial seawater, *Electrochimica Acta*, **314**, 135-141 (2019)
- 12. S. Schuerz, M. Fleischanderl, G. Luckeneder, K. Preis, T. Haunschmied, G. Mori, A. Kneissl, Corrosion behaviour of Zn–Al–Mg coated steel sheet in sodium chloride-containing environment, *Corrosion Science*, **51**(10), 2355-2363 (2009)
- 13. E.A. Esfahani, H. Salimijazi, M.A. Golozar, J. Mostaghimi, L. Pershin, Study of corrosion behavior of arc sprayed aluminum coating on mild steel, *Journal of thermal spray technology*, **21**(6), 1195-1202 (2012)
- 14. T.-Y. Yung, T.-C. Chen, K.-C. Tsai, W.-F. Lu, J.-Y. Huang, T.-Y. Liu, Thermal spray coatings of Al, ZnAl and inconel 625 alloys on SS304L for anti-saline corrosion, *Coatings*, **9**(1), 32 (2019)
- 15. P. Fauchais, A. Vardelle, Thermal sprayed coatings used against corrosion and corrosive wear, *Advanced plasma spray applications*, **10**, 34448 (2012)
- 16. R. M. H. Pombo Rodriguez, R.S.C. Paredes, S.H. Wido, A. Calixto, Comparison of aluminum coatings deposited by flame spray and by electric arc spray, *Surface and Coatings Technology*, **202**(1), 172-179 (2007)
- 17. E. Dalledone, M. Barbosa, S. Wolynec, Zinc-55% aluminum-1.6% silicon coating compared with zinc coating, *Materials performance*, **34**(7), (1995)
- 18. A. Marder, The metallurgy of zinc-coated steel, *Progress in materials science*, **45**(3), 191-271 (2000)
- Z. Panossian, L. Mariaca, M. Morcillo, S. Flores, J. Rocha, J. Pena, F. Herrera, F. Corvo, M. Sanchez,
 O. Rincon, Steel cathodic protection afforded by zinc, aluminium and zinc/aluminium alloy coatings in the atmosphere, *Surface and Coatings Technology*, 190(2-3), 244-248 (2005)
- 20. A. Gulec, O. Cevher, A. Turk, F. Ustel, F. Yilmaz, Accelerated corrosion behaviors of Zn, Al and Zn/15Al coatings on a steel surface, *Materiali in tehnologije*, **45**(5), 477-482 (2011)

- 21. Y. Li, Corrosion behaviour of hot dip zinc and zinc-aluminium coatings on steel in seawater, *Bulletin of Materials Science*, **24**(4), 355-360 (2001)
- 22. G. Kong, R. White, Toward cleaner production of hot dip galvanizing industry in China, *Journal of cleaner production*, **18**(10-11), 1092-1099 (2010)
- 23. S. Egtvedt, "Thermally Sprayed Aluminum (TSA) with Cathodic Protection as Corrosion Protection for Steel in Natural Seawater: Characterization of Properties on TSA and Calcareous Deposit," Institutt for materialteknologi, 2011
- 24. D. Mari, L. Miguel, C.E. Nebel, Comprehensive hard materials, Newnes, 2014
- 25. J.R. Davis, Handbook of thermal spray technology, ASM international, 2004
- 26. M.H. Abd Malek, N.H. Saad, S.K. Abas, N.M. Shah, Thermal arc spray overview, IOP Conference Series: Materials Science and Engineering, 2013, IOP Publishing, p 012028
- 27. R. Bolot, R. Bonnet, G. Jandin, C. Coddet, Application of CAD to CFD for the wire arc spray process, *Thermal Spray*, 889-894 (2001)
- 28. B. Syrek-Gerstenkorn, S. Paul, A.J. Davenport, Sacrificial thermally sprayed aluminium coatings for marine environments: A review, *Coatings*, **10**(3), 267 (2020)
- 29. S. Kuroda, J. Kawakita, M. Takemoto, An 18-year exposure test of thermal-sprayed Zn, Al, and Zn-Al coatings in marine environment, *Corrosion*, **62**(7), 635-647 (2006)
- 30. A. Güleç, Ö. Cevher, A. Türk, F. Ustel, F. Yılmaz, Accelerated corrosion behaviors of Zn, Al and Zn/15Al coatings on a steel surface, (2011)
- 31. L. Qiao, Y. Wu, J. Duan, W. Gao, S. Hong, Corrosion Behavior of Arc-Sprayed Pore-Sealed Zn and Al Coatings in Seawater Containing Sulfate-Reducing Bacteria (SRB), *Journal of Thermal Spray Technology*, **30**(6), 1557-1565 (2021)
- 32. S. Hong, Y. Wu, W. Gao, J. Zhang, Y. Qin, Corrosion behavior of arc-sprayed Zn-Al coating in the presence of sulfate-reducing bacteria in seawater, *Journal of Materials Engineering and Performance*, **24**(11), 4449-4455 (2015)
- 33. H. Katayama, S. Kuroda, Long-term atmospheric corrosion properties of thermally sprayed Zn, Al and Zn–Al coatings exposed in a coastal area, *Corrosion Science*, **76**, 35-41 (2013)
- 34. A.Q. Liu, K. Xiao, C.F. Dong, X.G. Li, Corrosion behaviour of Zn-Al pseudo-alloy coating on carbon steel in chloride environments, Advanced Materials Research, 2012, Trans Tech Publ, pp 45-48
- 35. H.-S. Lee, J.K. Singh, M.A. Ismail, C. Bhattacharya, A.H. Seikh, N. Alharthi, R.R. Hussain, Corrosion mechanism and kinetics of Al-Zn coating deposited by arc thermal spraying process in saline solution at prolong exposure periods, *Scientific reports*, **9**(1), 1-17 (2019)
- 36. H. Hu, P. Zhang, D. Wei, F. Su, Microstructure and corrosion behavior of arc sprayed Zn-xAl (x= 15, 30, 50) alloy coatings in NaCl solution, *Materials Research Express*, **6**(10), 1065f1067 (2019)
- 37. S. Djerourou, H. Lahmar, N. Bouhellal, Y. Mebdoua, Study of twin wire arc sprayed zinc/aluminum coating on low carbon steel substrate: application to corrosion protection, Advanced materials research, 2013, Trans Tech Publ, pp 271-276
- 38. A. Darabi, F. Azarmi, Investigation on Relationship Between Microstructural Characteristics and Mechanical Properties of Wire-Arc-Sprayed Zn-Al Coating, *Journal of Thermal Spray Technology*, **29**(1-2), 297-307 (2020)
- 39. H.-S. Lee, J.K. Singh, J.H. Park, Pore blocking characteristics of corrosion products formed on Aluminum coating produced by arc thermal metal spray process in 3.5wt.% NaCl solution, *Construction and Building Materials*, **113**, 905-916 (2016)
- 40. Q. Jiang, Q. Miao, W.-p. Liang, F. Ying, F. Tong, Y. Xu, B.-l. Ren, Z.-j. Yao, P.-z. Zhang, Corrosion behavior of arc sprayed Al–Zn–Si–RE coatings on mild steel in 3.5 wt% NaCl solution, *Electrochimica Acta*, **115**, 644-656 (2014)
- 41. A. B117, Standard Practice for Operating Salt Spray (Fog) Apparatus, *ASTM International (1997 Edition)*, (2011)

- 42. K. Geels, D.B. Fowler, W.-U. Kopp, M.R. ckert, Metallographic and materialographic specimen preparation, light microscopy, image analysis, and hardness testing, ASTM international West Conshohocken, 2007
- 43. Y. Meng, L. Liu, D. Zhang, C. Dong, Y. Yan, A.A. Volinsky, L.-N. Wang, Initial formation of corrosion products on pure zinc in saline solution, *Bioactive materials*, **4**, 87-96 (2019)
- 44. S. Tailor, A. Modi, S. Modi, Synthesis, microstructural, corrosion and antimicrobial properties of Zn and Zn–Al coatings, *Surface Engineering*, **35**(8), 736-742 (2019)
- 45. S.F. Bonabi, F. Ashrafizadeh, A. Sanati, S.M. Nahvi, Structure and corrosion behavior of arcsprayed Zn-Al coatings on ductile iron substrate, *Journal of Thermal Spray Technology*, **27**(3), 524-537 (2018)
- 46. A. Güleç, Ö. Cevher, F. Üstel, A. Türk, A. Akıncı, F. Yılmaz, Performance Comparison of Thermal-Sprayed Coatings for Ductile Iron Pipe, (2011)
- 47. A.R. Moreira, Z. Panossian, P.L. Camargo, M.F. Moreira, I.C.d. Silva, J.E.R. de Carvalho, Zn/55Al coating microstructure and corrosion mechanism, *Corrosion Science*, **48**(3), 564-576 (2006)
- 48. H. Dingyong, G. Dandan, J. Jianmin, Corrosion behavior of arc sprayed aluminum coating on magnesium alloy in chlorine ion [J], *Welding & Joining*, **3**, (2007)
- 49. C. Vargel, Corrosion of aluminium, Elsevier, 2020
- 50. V.S. Bagotsky, Fundamentals of electrochemistry, John Wiley & Sons, 2005
- 51. P. Marcus, Corrosion mechanisms in theory and practice, CRC press, 2011
- 52. H. Marchebois, S. Joiret, C. Savall, J. Bernard, S. Touzain, Characterization of zinc-rich powder coatings by EIS and Raman spectroscopy, *Surface and Coatings Technology*, **157**(2-3), 151-161 (2002)
- T. Nguyen, J. Hubbard, J. Pommersheim, Unified model for the degradation of organic coatings on steel in a neutral electrolyte, *JCT, Journal of coatings technology*, **68**(855), 45-56 (1996)
- 54. A. Goyal, H.S. Pouya, E. Ganjian, P. Claisse, A review of corrosion and protection of steel in concrete, *Arabian Journal for Science and Engineering*, **43**(10), 5035-5055 (2018)
- 55. Y. Liu, B.-s. Xu, Z.-x. Zhu, Z.-x. Li, J. Ma, New pattern Zn-Al-Mg-RE coating technics for steel structure sustainable design, *Journal of Central South University of Technology*, **12**(2), 211-214 (2005)
- 56. R. Landolfo, L. Cascini, F. Portioli, Modeling of metal structure corrosion damage: A state of the art report, *Sustainability*, **2**(7), 2163-2175 (2010)
- 57. G. Astm, Standard test method for conducting potentiodynamic polarization resistance measurements, *Annual Book of ASTM Standards*, **3**, 237-239 (2009)
- 58. A. Momber, P. Plagemann, V. Stenzel, Performance and integrity of protective coating systems for offshore wind power structures after three years under offshore site conditions, *Renewable energy*, **74**, 606-617 (2015)
- 59. B. Hinderliter, S. Croll, D. Tallman, Q. Su, G. Bierwagen, Interpretation of EIS data from accelerated exposure of coated metals based on modeling of coating physical properties, *Electrochimica acta*, **51**(21), 4505-4515 (2006)
- 60. A. López-Ortega, J. Arana, R. Bayón, Tribocorrosion of passive materials: A review on test procedures and standards, *International Journal of Corrosion*, **2018**, (2018)
- 61. F. Mansfeld, C. Tsai, Determination of coating deterioration with EIS: I. Basic relationships, *Corrosion*, **47**(12), 958-963 (1991)



Fig. 1. Wire arc spray gun showing the wire feedstock and air nozzles.

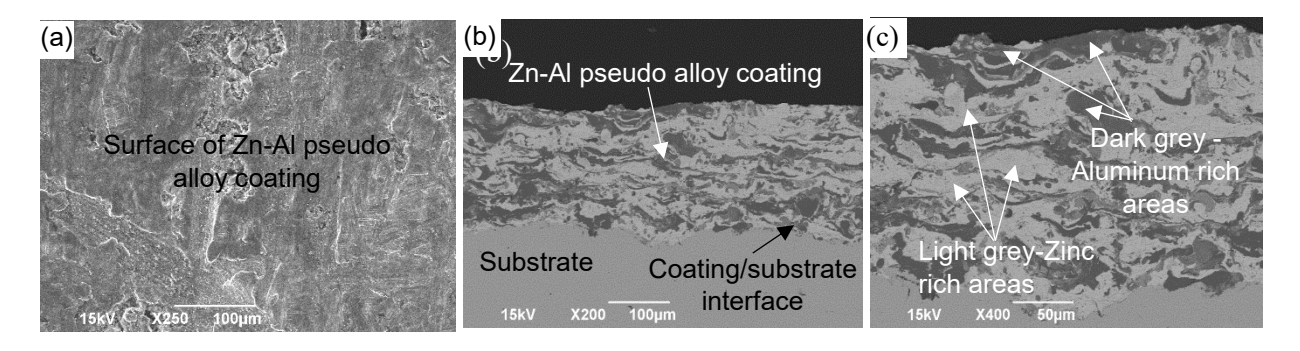


Fig. 2. Pseudo alloy coating: SEM micrograph of coating taken (a) on the surface at a magnification of ×250 (b) on the cross-section at low magnification (c) on the cross-section at a high magnification

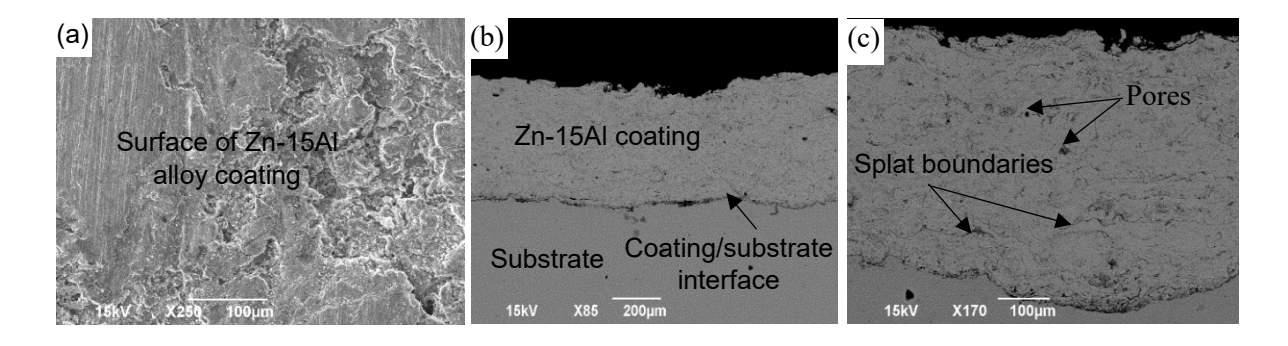


Fig. 3. Alloy coating: SEM micrograph of the coating taken (a) on the surface at a magnification of ×250, (b) on the cross-section at low magnification (c) on the cross-section at high magnification.

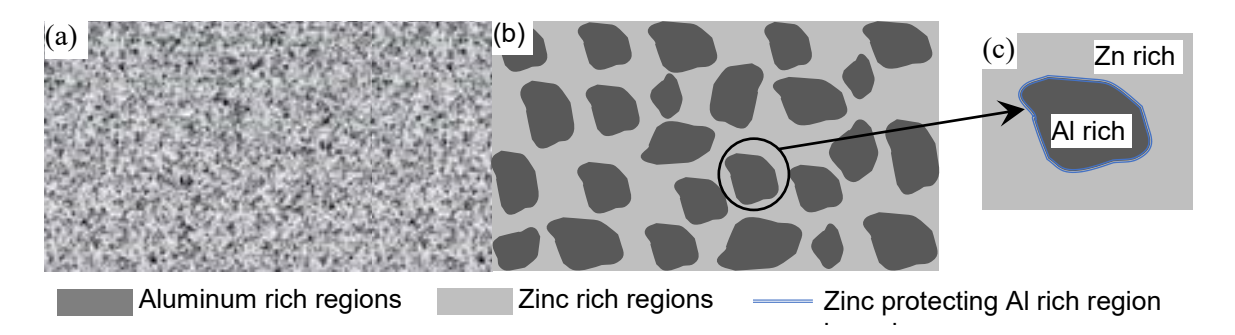


Fig. 4. Illustration of (a) Zn-Al alloy coating surface in which the Zn and Al are homogeneously distributed on the surface, (b) Zn-Al pseudo alloy in which the Zn- and Al-rich regions are visible on the surface, and (c) zinc sacrificially protecting the aluminum-rich region boundaries in pseudo alloy coatings which is not possible in Zn-15Al alloy coatings.

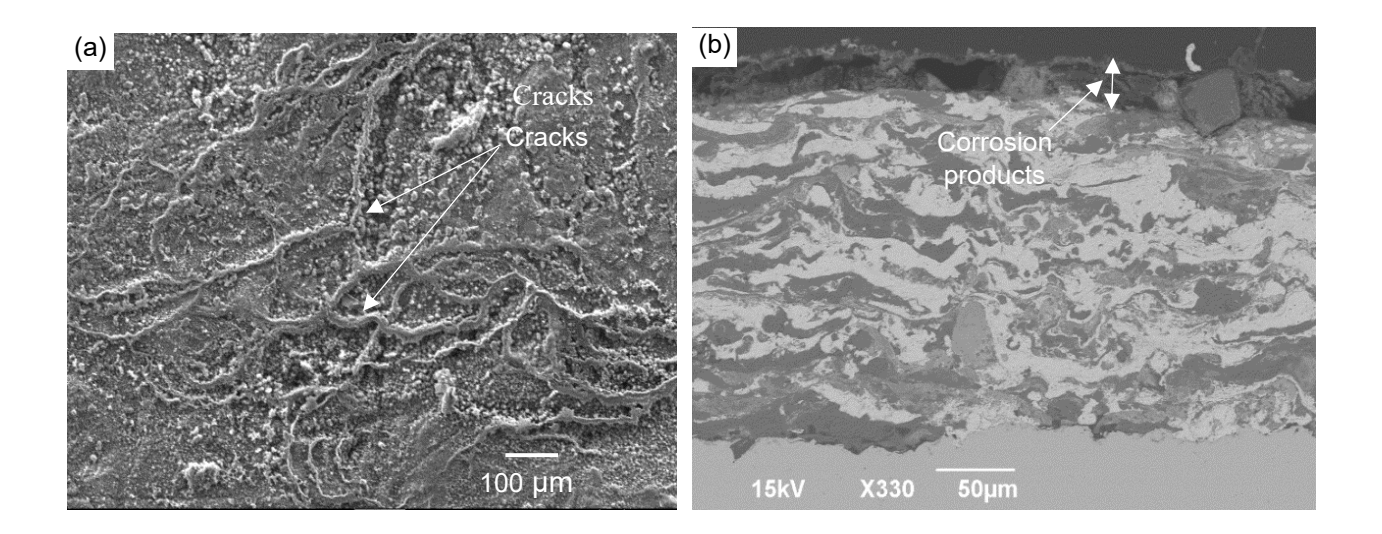


Fig. 5. Pseudo alloy coating: SEM micrograph of coating taken (a) on the surface (b) on the cross-section of Zn-Al pseudo alloy coating after being subjected to neutral salt spray.

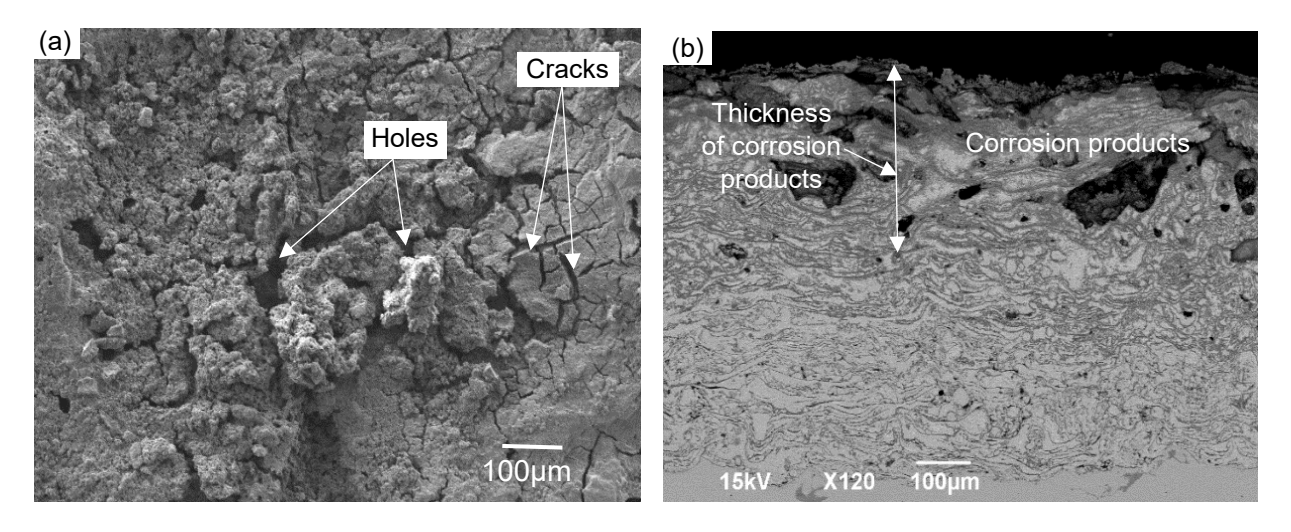


Fig. 6. Zn-15Al Alloy coating: SEM micrograph of coating taken (a) on the surface (b) on the cross-section of the Zn-15Al alloy coating after being subjected to neutral salt spray.

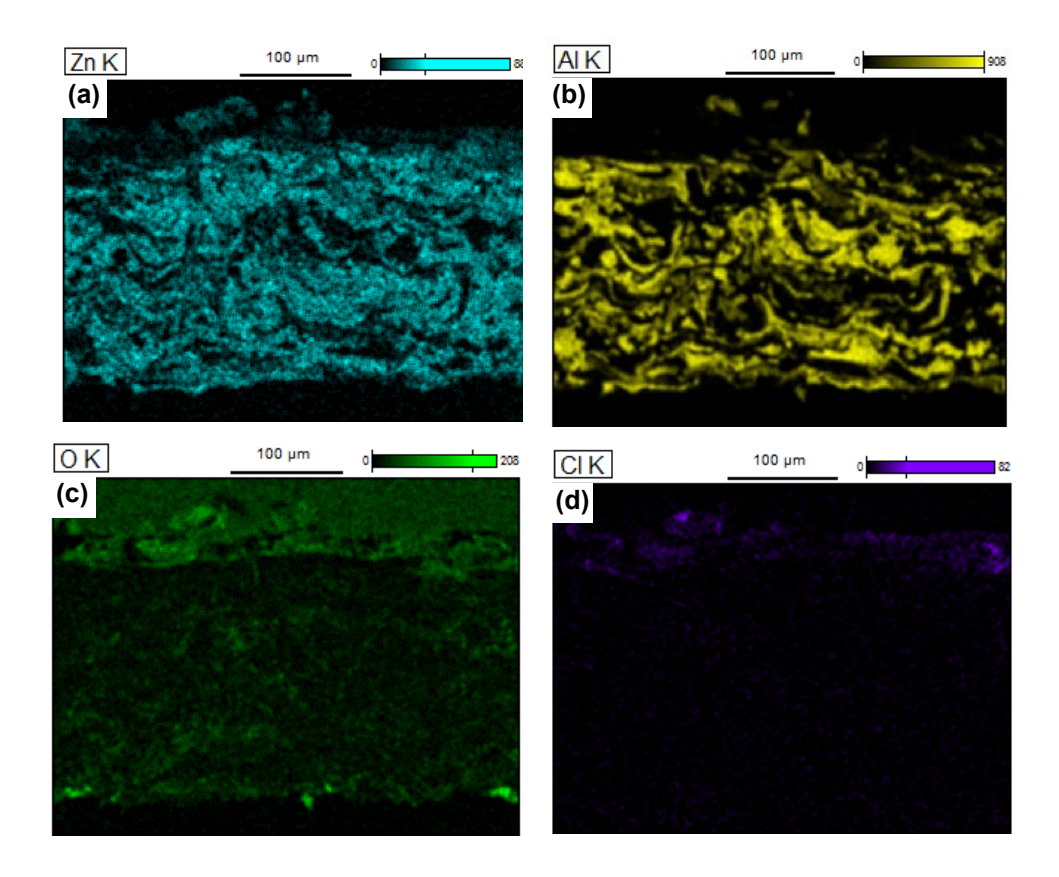


Fig. 7. Pseudo alloy coating: EDS map of the element (a) zinc (b) aluminum (c) oxygen and (d) chloride ion in the cross-section of Zn-Al pseudo alloy coating after being subjected to neutral salt spray.

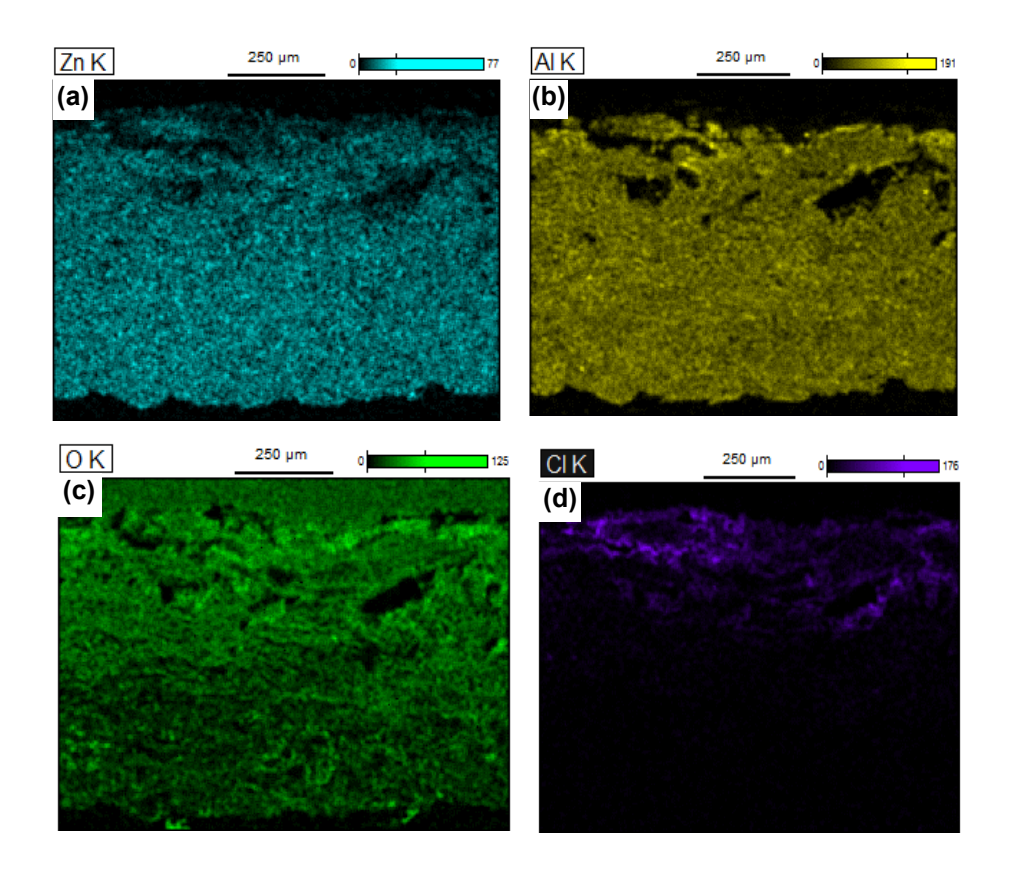


Fig. 8. Zn-15Al coating: EDS map of the element (a) zinc (b) aluminum (c) oxygen and (d) chloride ion in the cross-section of Zn-15Al coating after being subjected to neutral salt spray.

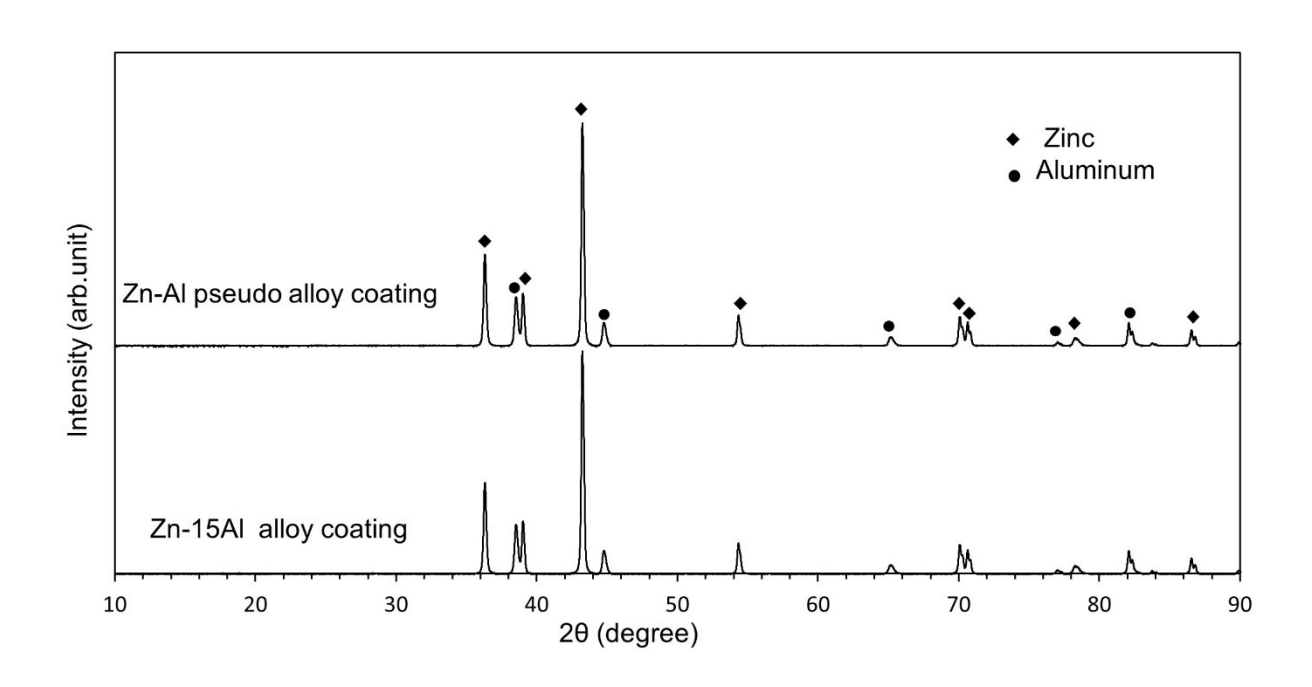


Fig. 9. XRD pattern obtained from the pseudo alloy and Zn-15Al coatings in as-deposited condition.

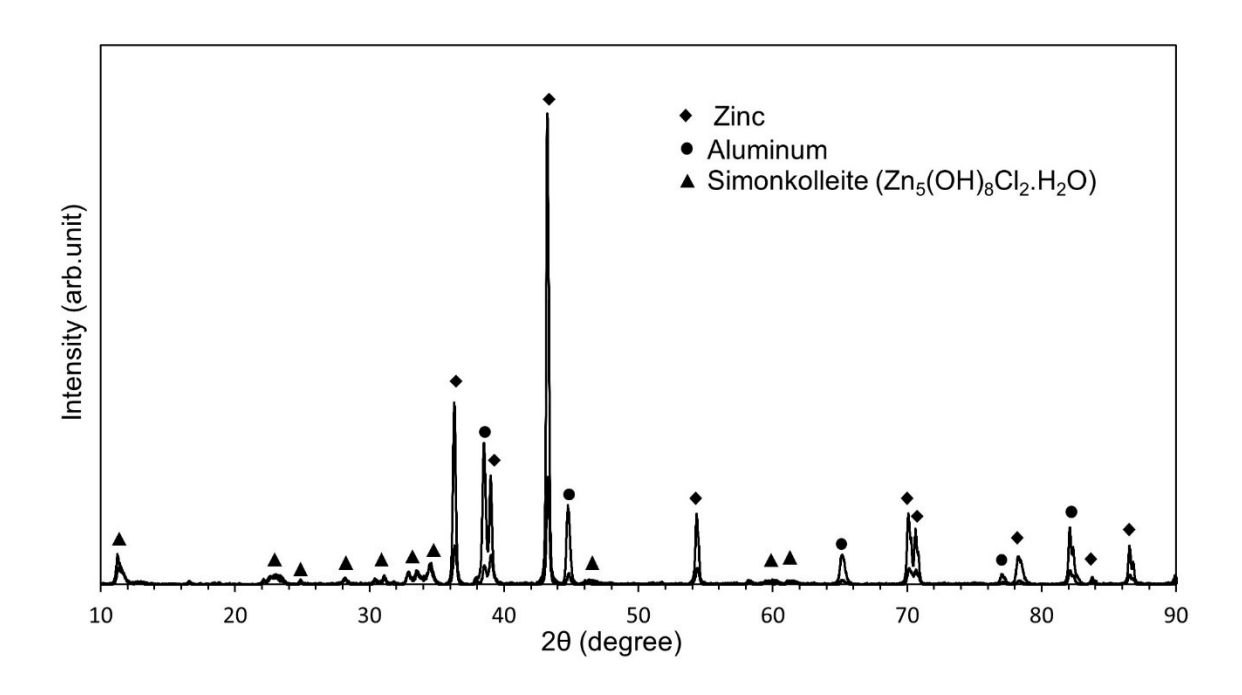


Fig. 10. XRD pattern of the corrosion products formed on the pseudo alloy coating after being subjected to neutral salt spray.

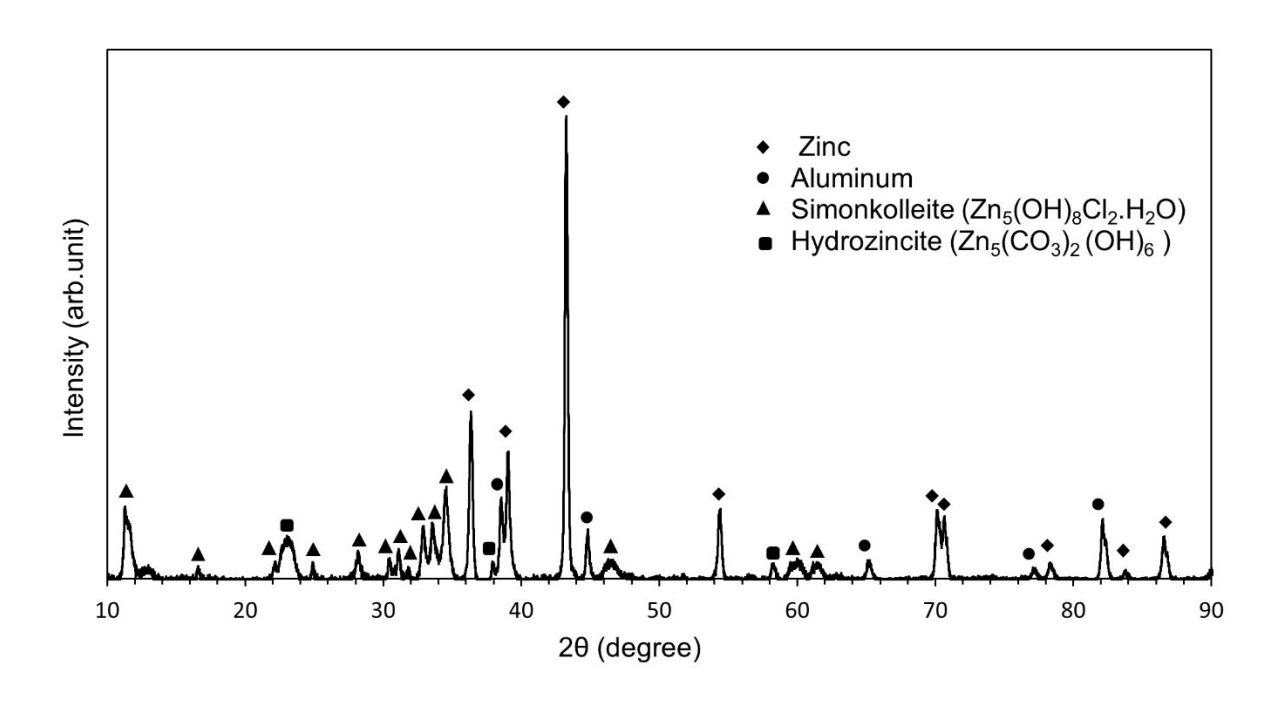


Fig. 11. XRD pattern of corrosion products formed on the Zn-15Al coating after being subjected to neutral salt spray.

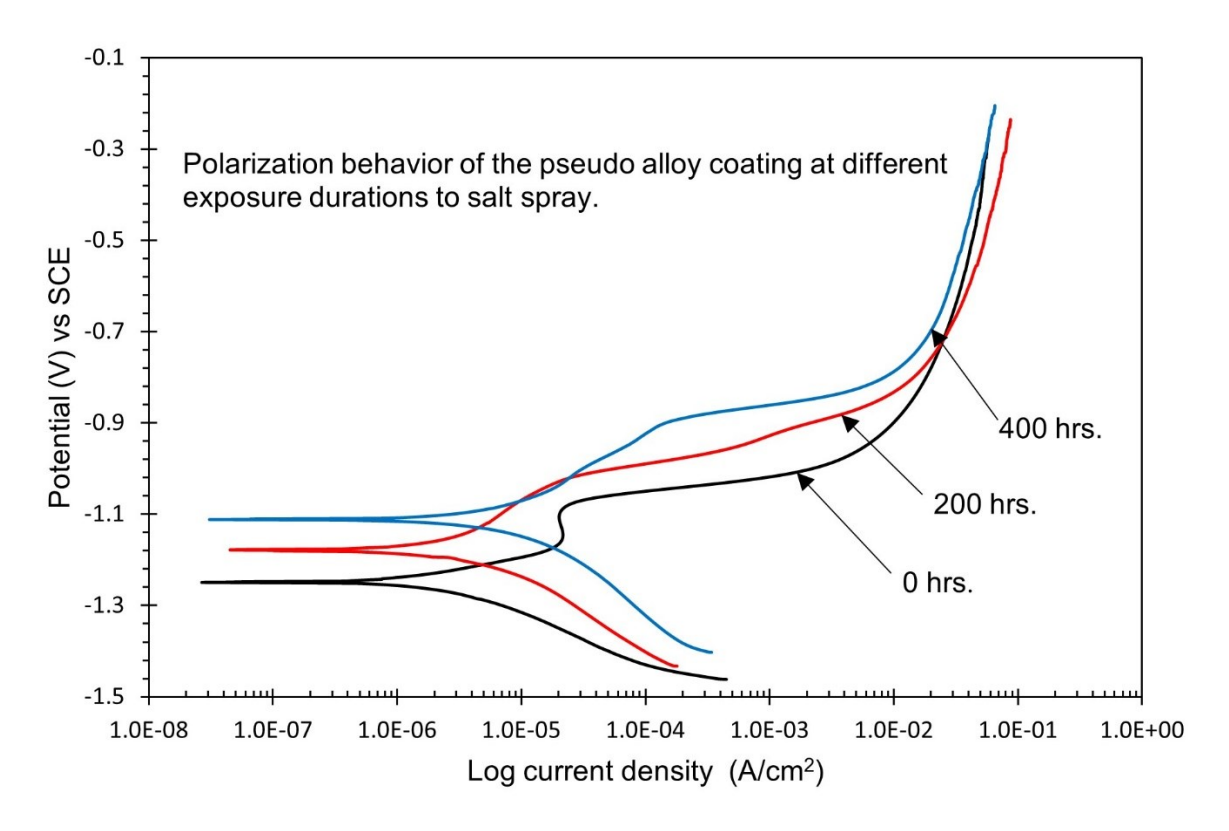


Fig. 12. Polarization curves of pseudo alloy coating at 0 hrs. 200 hrs. and 400 hrs. of neutral salt spray (3.5 wt.% NaCl) exposure.

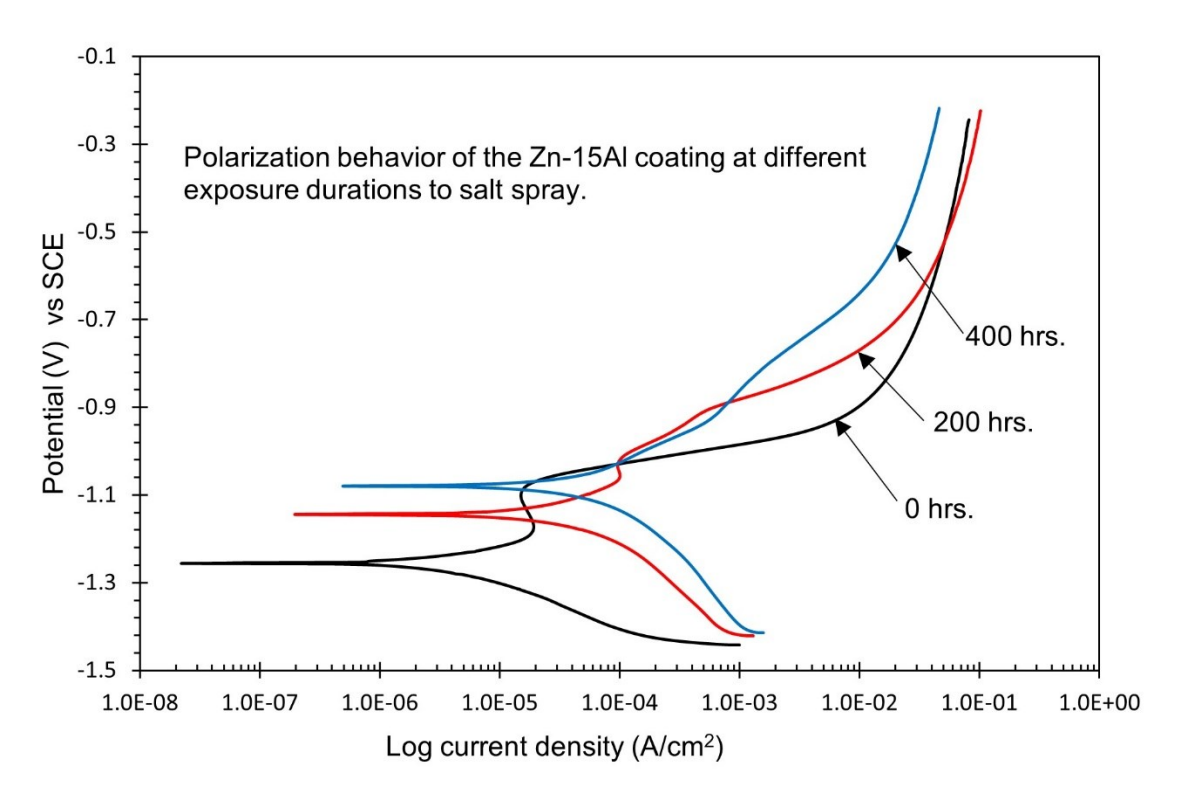


Fig. 13. Polarization curves of Zn-15Al coating at 0 hrs. 200 hrs. and 400 hrs. of neutral salt spray (3.5 wt.% NaCl) exposure.

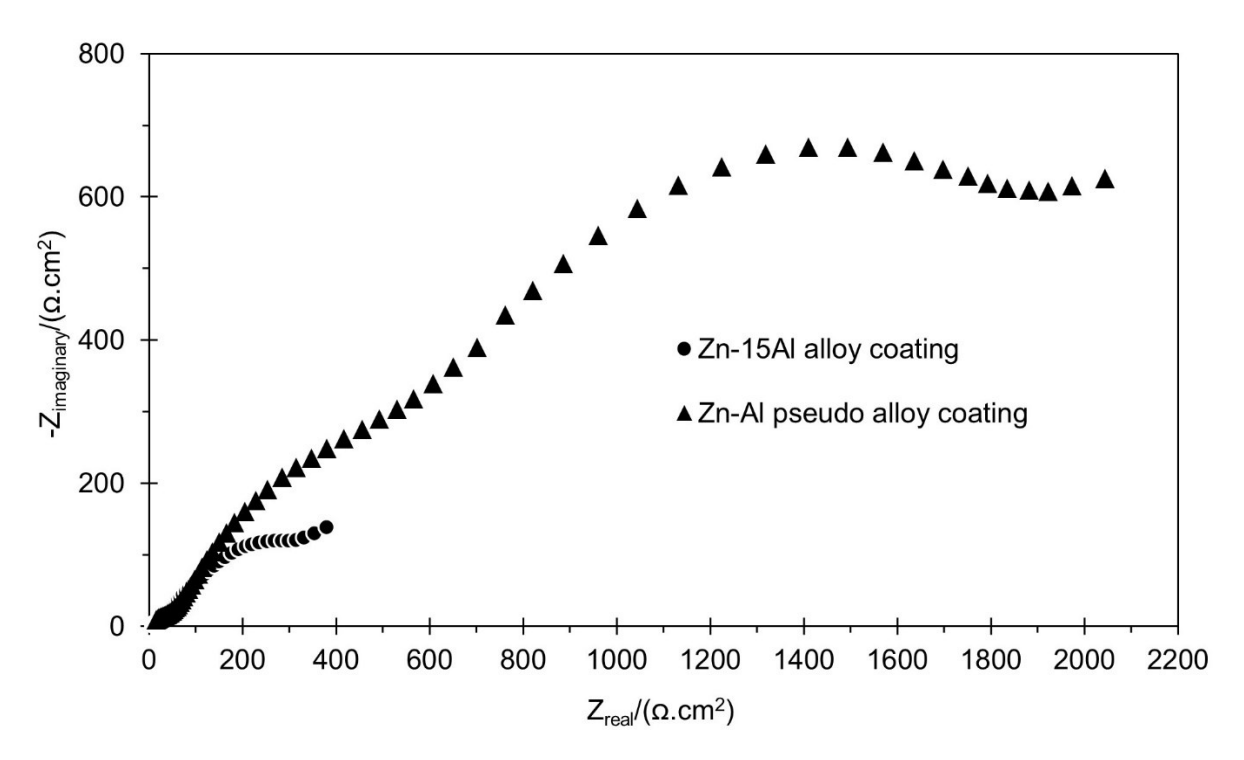


Fig. 14. Nyquist plot of the pseudo alloy and Zn-15Al coatings after being exposed to 400 hours of neutral salt spray.

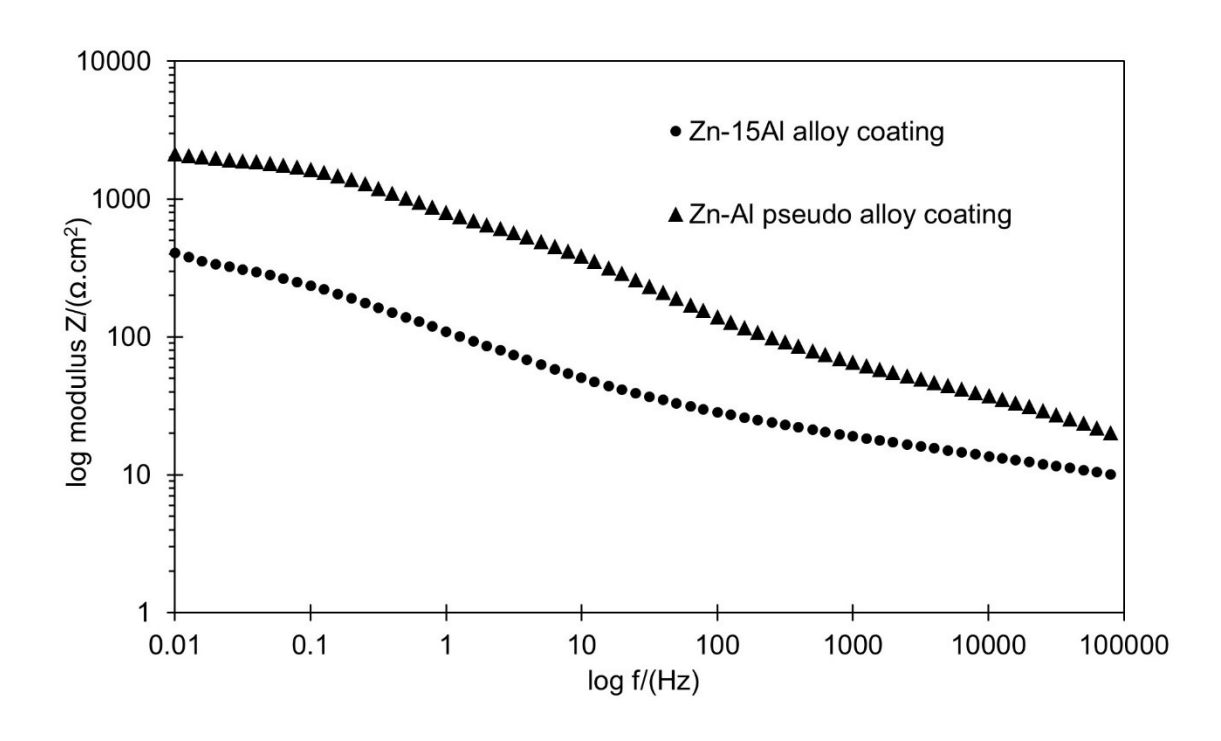


Fig. 15. Bode modulus plot of pseudo alloy and Zn-15Al coatings after being exposed to 400 hours of neutral salt spray.

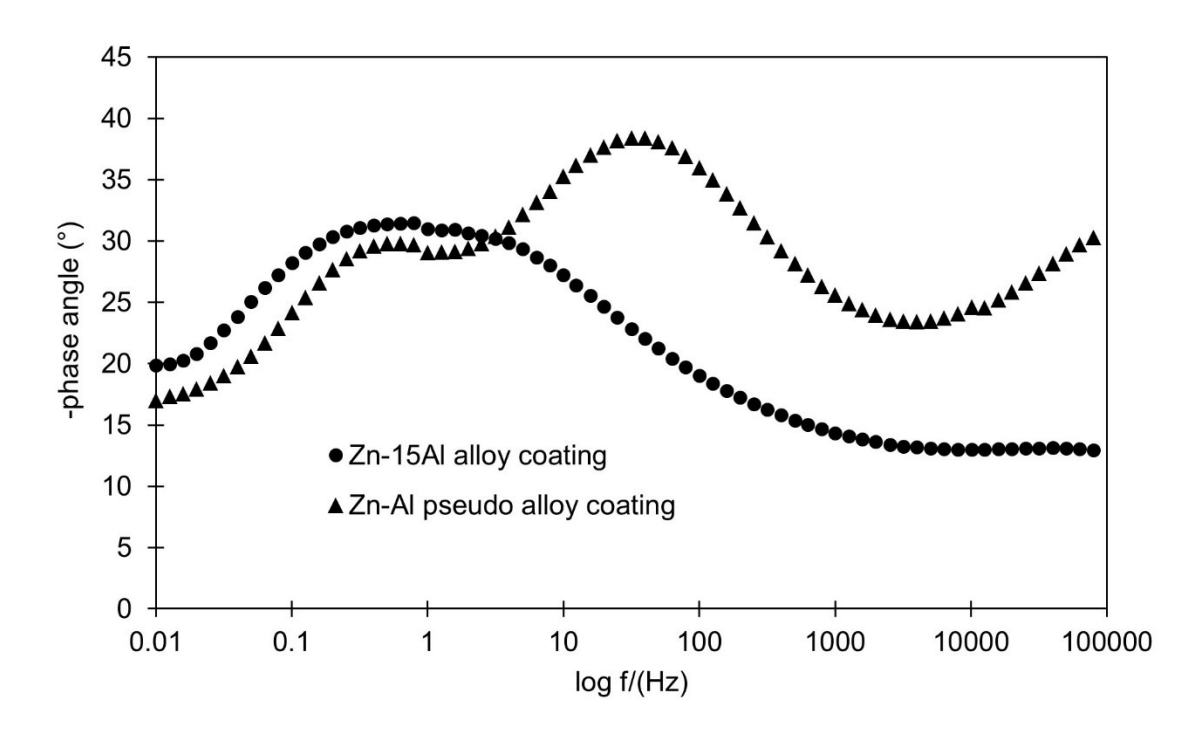


Fig. 16. Bode phase angle plot of the pseudo alloy and Zn-15Al coatings after being exposed to 400 hours of neutral salt spray.

Table 1. Wire arc spray process parameters.

Spray parameters	Value	
Spray distance	180 mm	
Current	150 Amps	
Voltage	32 Volts	
Pressurized gas	Air	
Inlet pressure	0.62 MPa	
Substrate temperature	Room temperature	

Table 2. Elemental composition of the coating obtained from EDS analysis

Coating type	Zinc, Wt.%	Aluminum, Wt.%	Oxygen, Wt.%
Zn-15Al alloy	79.78 ± 4.37	17.08 ± 0.41	3.15 ± 0.34
Zn-Al pseudo alloy	58.46 ± 3.60	37.21 ± 0.58	4.33 ± 0.33

Table 3. Electrochemical parameters obtained from Tafel extrapolation at different durations of neutral salt spray exposure.

Coating type	Salt spray exposure time (hours)	E _{corr} (V) vs SCE	i_{corr} $(\mu A/cm^2)$	Corrosion rate (µm/year)
	0	-1.26	4.53	65.83
Zn-15Al alloy	200	-1.14	41.00	-
	400	-1.08	136.00	-
	0	-1.25	1.17	16.60*
Zn-Al pseudo alloy	200	-1.18	7.30	-
	400	-1.11	3.40	-

^{*}The corrosion rate of pseudo alloy coating is calculated using the weighted average of mass fractions of zinc and aluminum obtained from EDS analysis.